Communications in Mathematics and Applications
Vol. 14, No. 2, pp. 901–914, 2023
ISSN 0975-8607 (online); 0976-5905 (print)
Published by RGN Publications
DOI: 10.26713/cma.v14i2.2084

http://www.rgnpublications.com

Research Article

Mathematical Analysis of Thermophoresis and Chemical Reaction Effect on Micropolar Fluid Flow in the Presence of Nano Particles

N. Golden Stepha*[1], G. Nixon Samuel Vijayakumar[2] and K. Muralidharan[3]

[1] *Department of Mathematics, R.M.K. Engineering College (affiliated to Anna University), Tiruvallur, Tamil Nadu, India*
[2] *Department of Physics, R.M.K. Engineering College (affiliated to Anna University), Tiruvallur, Tamil Nadu, India*
[3] *Department of Mechanical, R.M.K. Engineering College (affiliated to Anna University), Tiruvallur, Tamil Nadu, India*
***Corresponding author:** goldenstepha@gmail.com

Received: December 12, 2022 **Accepted:** May 1, 2023

Abstract. The present study focused on forced convective heat and mass transfer flow of viscous fluid in the presence of chemical reaction. A two-dimensional incompressible flow of a micropolar nanofluid past a continuously moving porous plate with variable viscosity is investigated. The viscous dissemination is considered in the energy condition. The governing boundary layer equation renovated into ODEs by considering similarity transformation. Numerical solution is obtained by adopting 4th order R-K numerical procedure together with NS shooting method. The impact of the parameters on the fluid concentration, temperature, velocity, and angular velocity are analyzed graphically for nano particle volume fraction $(0 < \phi < 2)$. The results of the flow model for different flow factors are exactly in line with the flow's physical conditions. It is explored that the increase in nano particle volume fraction ϕ causes decline in both microrotation and velocity of the fluid close to the boundary and for increasing thermophoretic parameter, both species concentration and fluid temperature decreases. The fluid's velocity and rotational velocity are lower in the solution with higher density nano particles.

Keywords. Nanofluid, Thermophoresis, Boundary layer, Micropolar fluid, Chemical reaction

Mathematics Subject Classification (2020). 35Q30, 35Q35, 35Q79

1. Introduction

Novel engineering materials named nanofluids contain colloidal nano particles suspended in a base fluid as invented by Choi *et al*. [3]. Notable applications include heat transfer from electronic circuits, geothermal electricity generation, nuclear reactors and MEMS/NEMS devices (Tyler *et al*. [17]). A low thermal conductivity coefficient is desirable in case of a base fluid. Commonly used materials as base fluids are alcohol, water, oil, and glycol ethylene. These fluids are made up of regular fluid and nanoparticles with diameters ranging from 10 nm to 100 nm that are uniformly mixed with the fluid. They usually contain particles of materials like Al_2O_3, TiO_2, Cu, and Ag. Nanoparticles suspended in base fluids offer enhanced thermal efficiency in terms of conductivity, diffusivity and consistency. Yu *et al*. [18] has comprehensively reviewed the role of nanofluids in the thermal transfer applications.

Das *et al*. [5], Choi *et al*. [4], and Liu *et al*. [9] have shown that the thermo-physical properties can be elevated by nanofluids. It is significant to explore the flow of micro polar fluid in the boundary layer on a surface that is continually moving in the crystal growth process. Cemel [2] initiated the concept of micro polar fluid. The heat transfer effect of micro polar fluid over a continuously moving plate was studied elaborately (Soundalgekar and Takhar [16], and Rapits [14]).

Fluid viscosity measures the internal resistance to the fluid flow which is a degree of the internal stickiness of the fluid. Extensive research on heat transfer in fluid flow has shown that viscosity is taken to be constant if the temperature difference is small. An increase in oil temperature due to internal resistance changes the viscosity and is not constant over a period of time. Therefore to forecast the flow behavior accurately, we should assume viscosity as a variable quantity significantly. Therefore, in the present work the fluid viscosity of the micro polar nanofluid is considered to vary with respect to temperature and it varies in a linear manner.

Several physical problems deal with the combined effect of moving fluid with radiation. Loganathan and Stepha [11, 10] considered the problem of heat and mass transfer outcomes of the forced convective flow of radiative micro polar fluid. Jeevandhar *et al*. [8] studied free convective flow of micro polar nanofluid over a shrinking sheet. Singh *et al*. [15] put forward their work on micro polar fluid flow through stretchable surface with chemical reaction and melting heat transfer. Rafique *et al*. [13] considered micro polar nanofluid over an inclined surface and presented numerical solution using Keller Box method. Fatunmbi and Salawu [6] analyzed hydro magnetic micro polar nanofluid flow past a stretchy nonlinear sheet.

Thermophoresis is an interesting term wherein a little micron estimated molecule suspended in a gas moving with the speed toward diminishing thermal gradient.

Brownian motion and thermophoresis characteristics on a radiative reactive micro polar fluid flow over a moving flat plate constantly is analyzed by Mabood *et al*. [12] and solution is presented using HAM. Hazarika and Ahmed [7] explained the material behavior in micro polar fluid of Brownian motion over a stretchy disk with application of thermophoretic forces and diffusion.

The contemporary article intends to investigate the impact of thermophoresis and mass transfer on a micro polar suspensions in nanofluidics model, in particular water solution of Al_2O_3, TiO_2, Cu and Ag past a continuously moving penetrable plate in the presence of chemical reaction.

2. Materials and Methods

A forced convective flow on a constantly shifting permeable horizontal sheet with a continual velocity in a water-primarily based nanofluid which is at rest and contains distinct nanoparticles including TiO_2, Cu, Ag and Al_2O_3 is modeled mathematically. Flow is supposed to be steady, two-dimensional, and incompressible. As shown in Figure 1 shows that the source of the structure is positioned wherein the is brought into the liquid medium.

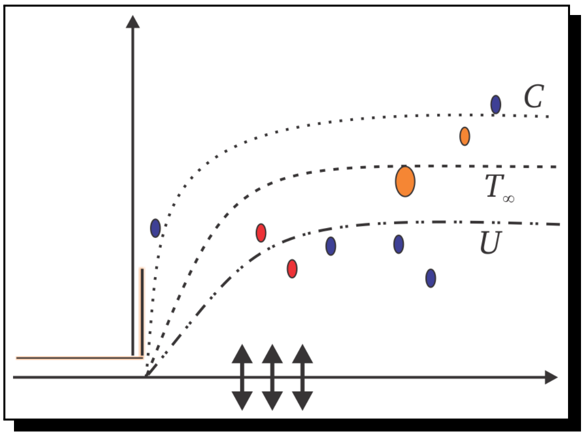

Figure 1. Flow pattern

The uniform temperature T_W is maintained at the surface of the plate. The uniform concentration C_W is maintained at the outward of the plate. The properties of the fluid such as time-dependent fluid viscosity, gray, and emitting are taken into description.

Table 1. Characteristics of nanoparticles

Nano particles	Physical properties		
	ρ(kg/m^3)	C_p(j/kg)K	K(W/mK)
Al_2O_3	3970	765	40
TiO_2	4250	686.2	8.9538
CuO (Copper Oxide)	6320	531.8	76.5
Cu (Copper)	8933	385	400
Ag (Sliver)	10500	235	429

2.1 Governing Equations

The equations governing the boundary layer flow are

$$\frac{\partial u}{\partial x}+\frac{\partial v}{\partial y}=0, \tag{2.1}$$

$$u\frac{\partial u}{\partial x}+v\frac{\partial v}{\partial y}=\frac{1}{\rho_{nf}}\frac{\partial}{\partial y}(\mu_{nf}+k)\frac{\partial u}{\partial y}+\frac{k}{\rho_{nf}}\frac{\partial \sigma}{\partial y}, \tag{2.2}$$

$$\rho_{nf}j\left(u\frac{\partial \sigma}{\partial x}+v\frac{\partial \sigma}{\partial y}\right)=\gamma_{nf}\frac{\partial^2 \sigma}{\partial y^2}-k\left(2\sigma+\frac{\partial u}{\partial y}\right), \tag{2.3}$$

$$u\frac{\partial T}{\partial x}+v\frac{\partial T}{\partial y}=\frac{k_{nf}}{(\rho c_p)_{nf}}\frac{\partial^2 T}{\partial y^2}+\frac{\gamma_{nf}}{c_p}\left(\frac{\partial u}{\partial y}\right)^2-\frac{1}{(\rho c_p)_{nf}}\left(\frac{\partial q_r}{\partial y}\right), \tag{2.4}$$

$$u\frac{\partial C}{\partial x}+v\frac{\partial C}{\partial y}=D\frac{\partial^2 C}{\partial y^2}-R_C(C-C_\infty)-\frac{\partial}{\partial y}(V_T(C-C_\infty)). \tag{2.5}$$

Subjected to the boundary conditions,

$$\left.\begin{aligned} &u=U_0,\ v=V_W,\ \sigma=-n\tfrac{\partial u}{\partial y},\ T=T_W,\ C=C_W \text{ as } y\to 0\\ &u=0,\ v=0,\ \sigma=0,\ T=T_\infty,\ C=C_\infty \text{ as } y\to\infty \end{aligned}\right\} \tag{2.6}$$

where

$$\rho_{nf}=(1-\phi)\rho_f+\phi\rho_s,$$

here volume fraction of nano-solid particle, density of the base fluid, density of nanofluid, and the density of the solid particle are denoted by ϕ, ρ_f, ρ_{nf}, ρ_s, respectively.

$$(\rho c_p)_{nf}=(1-\phi)(\rho c_p)_f+\phi(\rho c_p)_s,$$

$$\mu_{nf}=\frac{\mu_f}{(1-\phi)^{2.5}},\ V_T=-\frac{k_T v_f}{T_\infty}\frac{\partial T}{\partial y}$$

Now let us consider dimensionless variables,

$$\eta=y\sqrt{\frac{U_0}{2\gamma_f x}},\ \ \psi=\sqrt{2\gamma_f U_0 x}f(\eta),$$

$$\sigma=\sqrt{\frac{U_0^3}{2\gamma_f x}}g(\eta),\ \ \theta=\frac{T-T_\infty}{\Delta T},\ \ \varphi=\frac{C-C_\infty}{\Delta C}, \tag{2.7}$$

where

$$\Delta T=T_W-T_\infty,\ \ \Delta C=C_W-C_\infty$$

$$Pr=\frac{\gamma_f\rho c_\rho}{k},\ \ N=\frac{k'k_{nf}}{4\sigma_1 T_\infty^3},\ \ Ec=\frac{U_0^2}{c_p(T_W-T_\infty)},$$

$$F_W=-V_W\sqrt{\frac{2x}{\gamma_f U_0}},\ \ T_V=-\frac{k_T(T_W-T_\infty)}{T_\infty},$$

where non-dimensional stream functions are $f(\eta)$ and $g(\eta)$, using the above defined dimensionless variables (2.7), equations (2.2)-(2.5) are renewed to the following system of equations:

$$\frac{\left(\frac{\mu_{nf}}{\mu_f}+k\right)}{\left((1-\phi)+\phi\frac{\rho_s}{\rho_f}\right)}f'''+ff''+\frac{\gamma_r}{(1-\phi)^{2.5}\left((1-\phi)+\phi\frac{\rho_s}{\rho_f}\right)}f''\theta'+\frac{k}{\left((1-\phi)+\phi\frac{\rho_s}{\rho_f}\right)}g'=0, \tag{2.8}$$

$$\frac{\left(\frac{\mu_{nf}}{\mu_f}+\frac{k}{2}\right)}{\left((1-\phi)+\phi\frac{\rho_s}{\rho_f}\right)}g''-gf'+fg'+\frac{2k}{\left((1-\phi)+\phi\frac{\rho_s}{\rho_f}\right)}(2g+f'')=0, \tag{2.9}$$

$$(3N+4)\theta''+\frac{3NPrEc}{(1-\phi)^{2.5}\left((1-\phi)+\phi\frac{\rho_s}{\rho_f}\right)}(f'')^2+3NPrf\theta'=0, \tag{2.10}$$

$$\frac{1}{(1-\phi)^{2.5}\left((1-\phi)+\phi\frac{\rho_s}{\rho_f}\right)}\lambda''+Sc\lambda'f+ScR\lambda-\frac{1}{(1-\phi)^{2.5}\left((1-\phi)+\phi\frac{\rho_s}{\rho_f}\right)}T_V Sc(\lambda\theta''+\theta'\lambda')=0. \tag{2.11}$$

The equivalent initial and boundary conditions in dimensionless quantities are

$$\left.\begin{array}{l} f(0)=F_W,\ f'(0)=1,\ g(0)=-nf'',\ \theta(0)=1,\ \lambda(0)=1 \text{ as } \eta=0,\\ f'(\infty)=0,\ g(\infty)=0,\ \theta(\infty)=0,\ \lambda(\infty)=0 \text{ as } \eta=\infty. \end{array}\right\} \tag{2.12}$$

3. Results and Discussion

The equation governs the present model and its boundary conditions are solved with the aid of the usage of the 4th order R-K and shooting techniques (Adams and Rogers [1]) for the cautioned parameters volume fraction of nano-solid particle ϕ, suction or injection Parameter Fw, coupling constant K, radiation parameter N, Prandtl number Pr, Schmidt number Sc, and thermophoresis parameter Tv. A program become created for the NS shooting approach along with 4th order R-K approach to resolve the equations (2.7)-(2.10) with boundary situation (2.11). Further the convergence criterion of 10^{-4}, fulfilled at all points in all circumstances, for the step size of $\Delta\eta = 0.01$. The main focus of the research was on the effects that occur in nanofluids. The following homogeneous water solutions of nanoparticles were investigated in this study:

- Al_2O_3 nanoparticles in a water solution
- TiO_2 nanoparticles in a water solution
- Cu nanoparticles in a water solution
- Ag nanoparticles in a water solution

The numerical evaluations for dimensionless velocity, microrotation, temperature and concentration are processed for the succeeding general values $K = 2$, $Pr = 0.7$, $EC = 0.02$, $N = 5.0$, $SC = 1.0$, $R = 0.4$, $\Upsilon_f = 0.8$, $Tv = 0.3$ and $n = 0.5$. Figures 2-5 shows the velocity, microrotation, temperature and concentration distribution for different nano particles Al_2O_3, TiO_2, Cu and Ag. The fluid's velocity, concentration, temperature, and rotational velocity are lower in the solution with higher density nano particles.

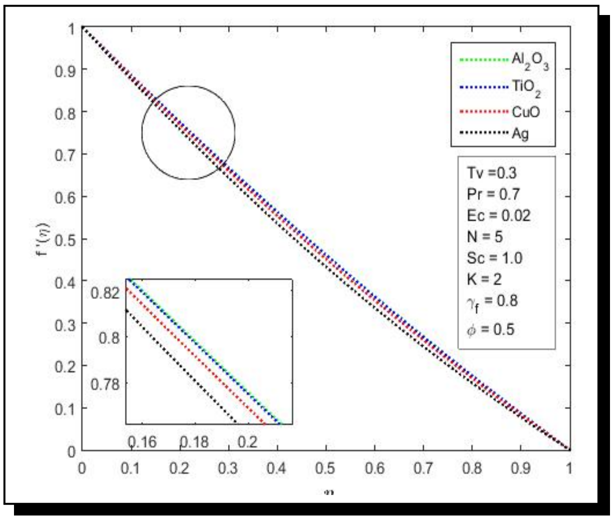

Figure 2. Velocity of the fluid for various nano particle types

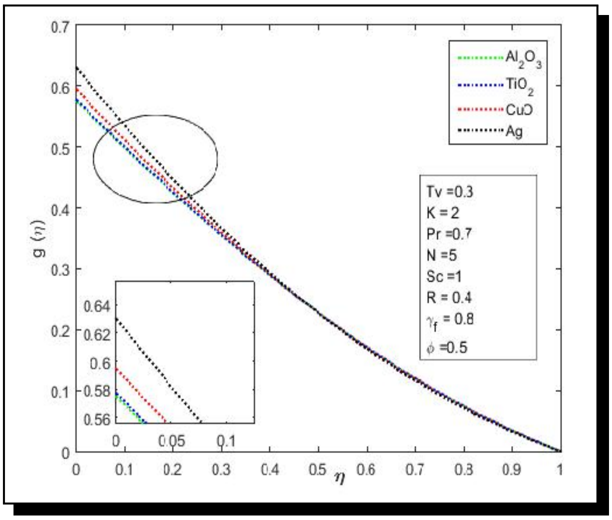

Figure 3. Angular velocity of the fluid for different nano particles

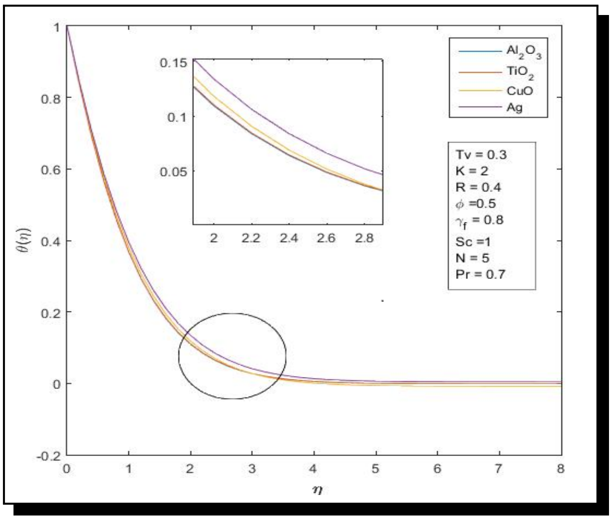

Figure 4. Temperature of the fluid for different nano particles

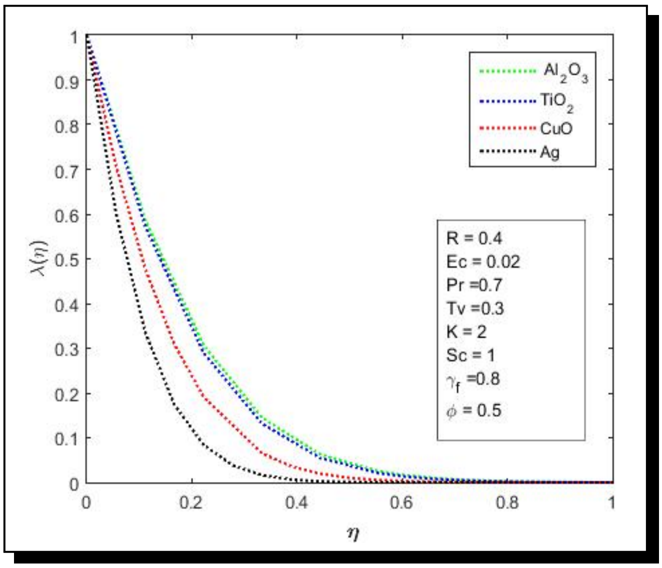

Figure 5. Concentration of the fluid for different nano particles

The velocity and angular velocity of the fluid close to the boundary layer for various values of coupling constant K is described in Figure 6 and 7. It is noticed that the velocity and rotational velocity of the fluid decline for higher values of coupling constant.

The effects of different values of thermophoretic parameter on concentration of the fluid in boundary layer of the flow are shown graphically in Figure 8. It is detected that concentration boundary layer thickness declines for increasing value of thermophoretic parameter.

For various chemical reaction parameter R, the concentration profile of the fluid flow are shown in Figure 9. It has been noted that as R is increased, the fluid's concentration decreases. This is a result of the concentration of the liquid do not stays steady and is devoured ceaselessly over the span of response, so the concentration diminishes as R increases.

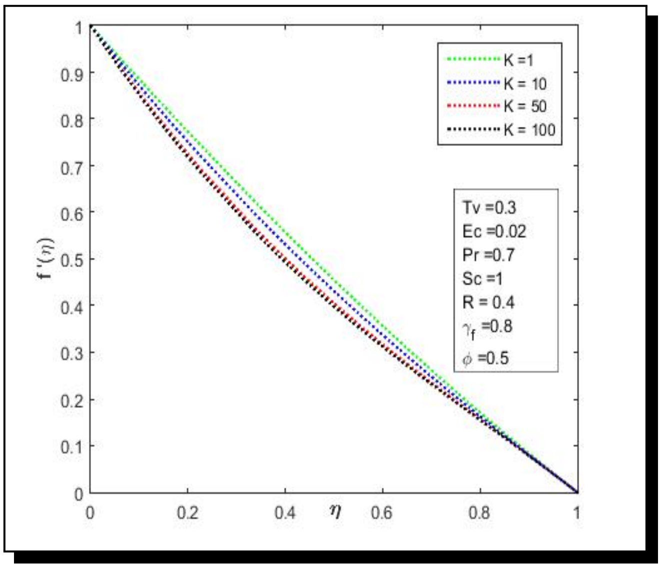

Figure 6. Velocity profile for different coupling constant

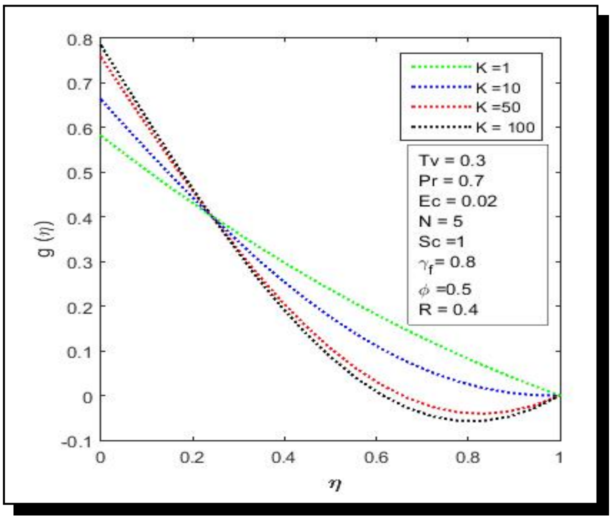

Figure 7. Angular Velocity profile for different coupling constant

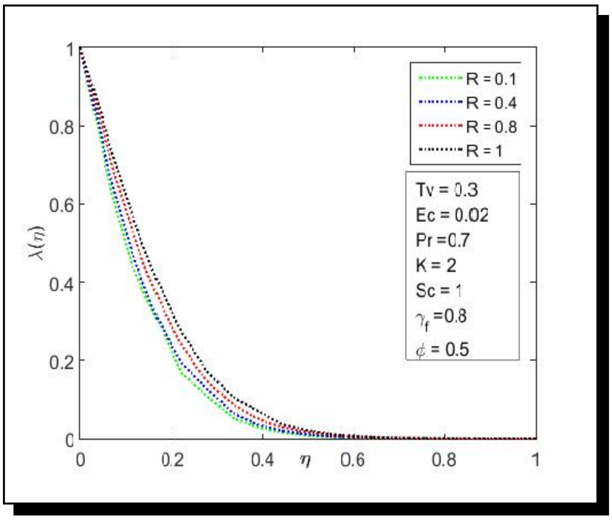

Figure 8. Concentration profile for different thermophoretic parameter

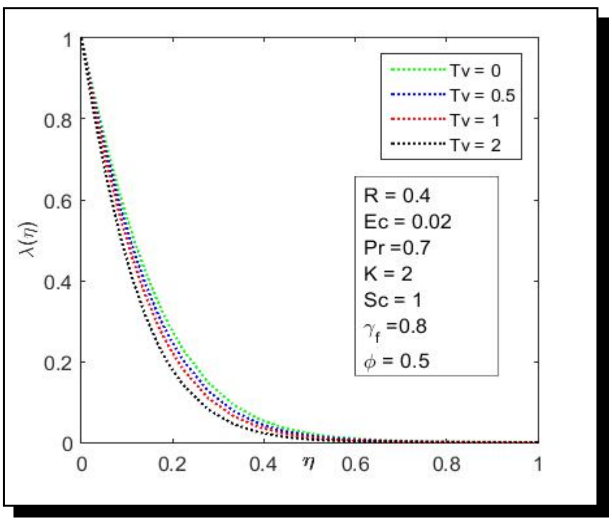

Figure 9. Influence of different chemical reaction on fluid concentration

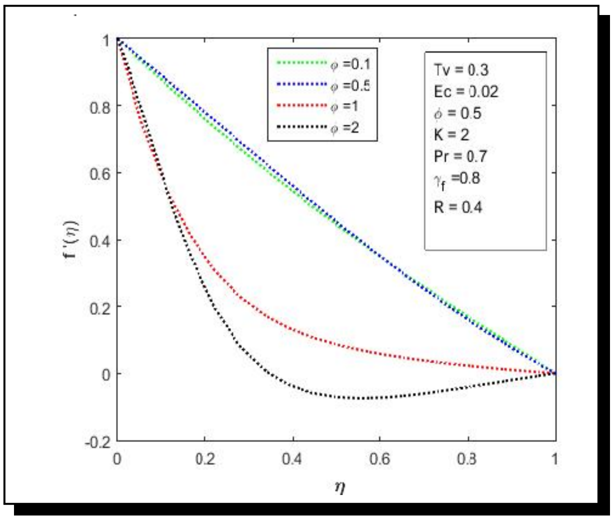

Figure 10. Influence of different φ on fluid velocity

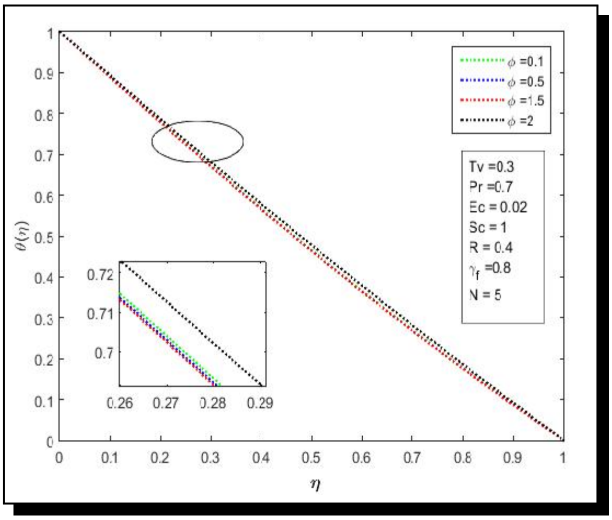

Figure 11. Influence of different φ on fluid temperature

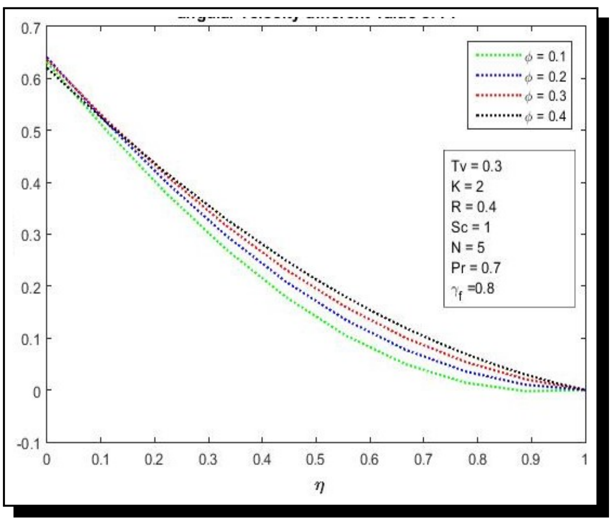

Figure 12. Effect of different φ on angular velocity of the fluid

Velocity field of the fluid is described in Figure 10 for $\varphi = 0.4, 0.3, 0.2, 0.1$ near the boundary layer of the flow. The fluid velocity declines as the volume fraction of nano-solid particles rises, as seen in Figure 10.

Figure 11 exhibits the temperature distribution of the micropolar nanofluid and it states a slight variation in the fluid temperature when the volume fraction of nano-solid particle changes.

Figure 12 depicts the angular velocity of the micropolar nanofluid near the boundary for various values of the volume fraction of nano-solid particles. The angular velocity of the micropolar nanofluid is seen to be decline as φ decreases.

Figure 13 exhibits the concentration distribution of the micropolar nanofluid and it states the concentration of the fluid drops when the volume fraction of nano-solid particle increases.

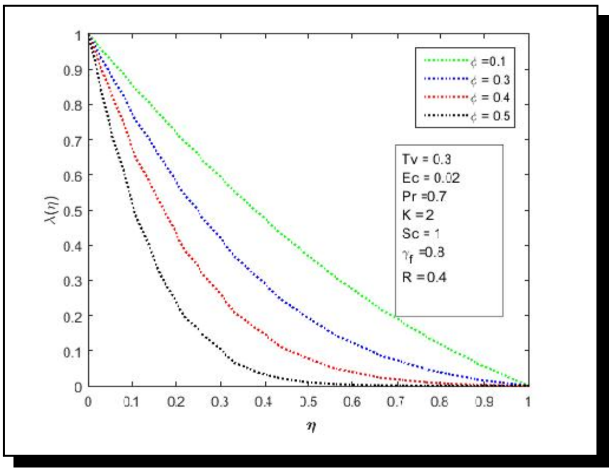

Figure 13. Influence of different φ on fluid concentration

The concentration distribution of the micropolar nanofluid for various Schmidt numbers is shown in Figure 14, and it can be seen that the fluid concentration drops as *Sc* increases.

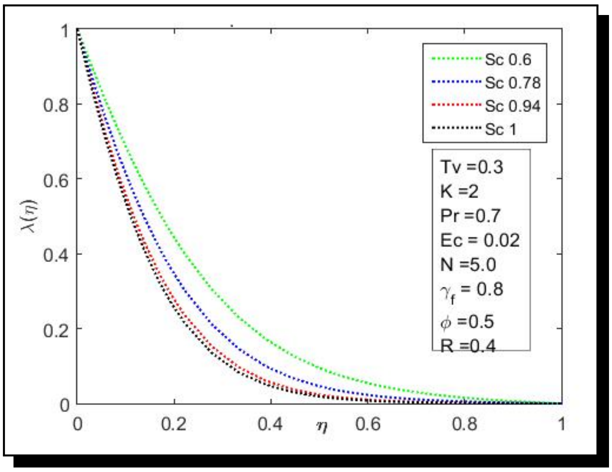

Figure 14. Influence of *Sc* on fluid Concentration

The temperature and concentration distributions of the micropolar nanofluid are shown in Figures 15 and 16 for various values of Pr, and it can be seen that the fluid temperature and concentration diminutions as Pr upsurges.

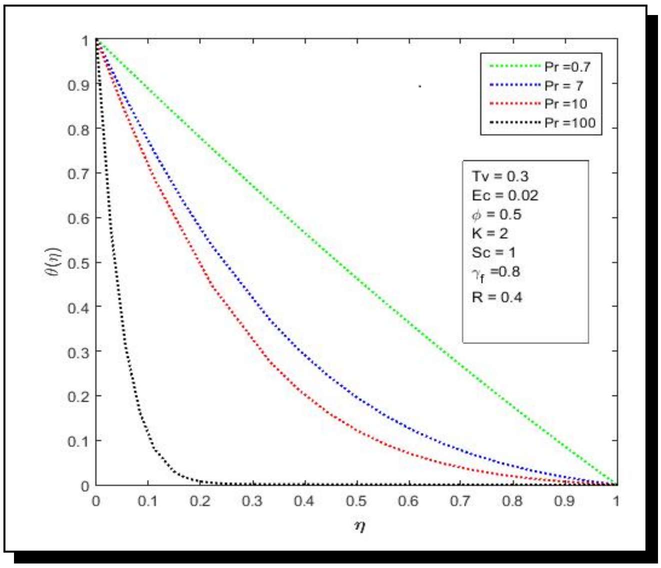

Figure 15. Impact of Prandtl number on fluid temperature

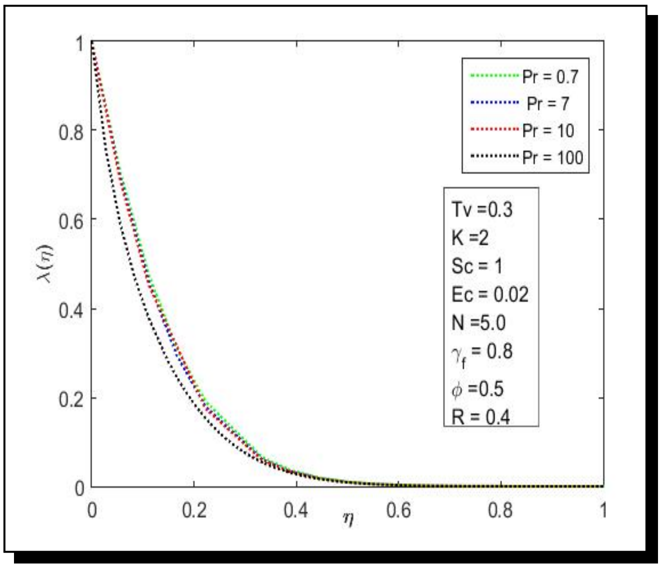

Figure 16. Impact of Prandtl number on fluid concentration

Figure 18 shows the mass transfer curve for various values of Sc at $Tv = 0$, demonstrating that higher values of Sc result in more mass transfer.

4. Conclusions

In the boundary layer, the influence of the micropolar nanofluid flow's velocity, microrotation, temperature, and concentration was examined numerically.

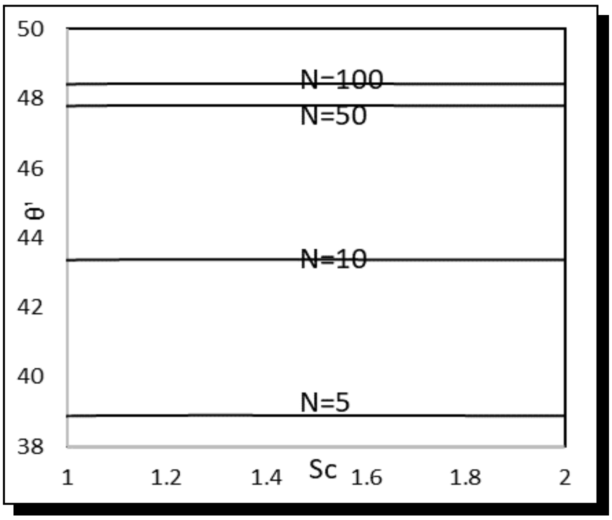

Figure 17. Heat transfer for different value for N

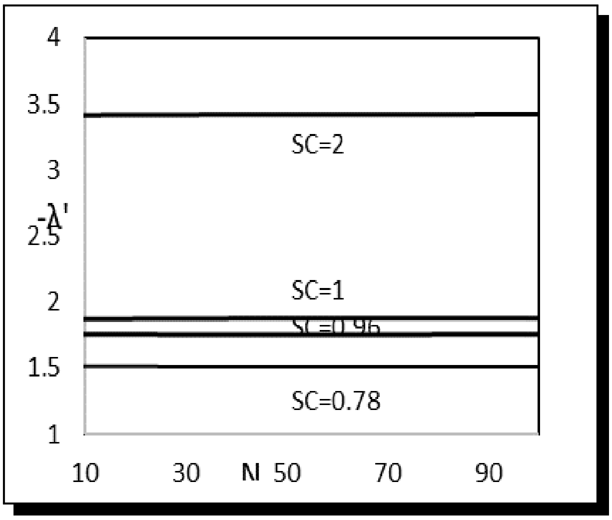

Figure 18. Impact of Schmidt number on mass transfer of the fluid

The computed parameters include the radiation parameter N, the volume fraction of nano-solid particles, Pr, and the Schmidt number. Additionally, a visual representation of the effects of the aforementioned parameters on the fluid's velocity, concentration, temperature, rotational velocity and within the boundary layer is shown.

Finally, it is concluded that:

- The fluid's velocity, concentration, temperature, and rotational velocity are lower in the solution with higher density nano particles.
- The fluid's velocity, concentration, temperature, and rotational velocity within the boundary layer reduces as the volume percentage of nano-solid particles grows.
- As the thermophoretic parameter and chemical reaction are increased, the concentration of the fluid falls.

- As the Prandtl number rises, the fluid temperature drops, and the fluid concentration drops as the Schmidt number rises.
- As *Pr* rises, so does the heat transfer coefficient, but as Schmidt number rises, so does the quantity of mass transfer.

Competing Interests

The authors declare that they have no competing interests.

Authors' Contributions

All the authors contributed significantly in writing this article. The authors read and approved the final manuscript.

References

[1] J. A. Adams and D. F. Rogers, *Computer-Aided Heat Transfer Analysis*, McGraw-Hill (1973).

[2] E. A. Cemal, Simple microfluids, *International Journal of Engineering Science* **2**(2) (1964), 205 – 207, DOI: 10.1016/0020-7225(64)90005-9.

[3] S. U. S. Choi, Nanofluids: from vision to reality through research, *ASME Journal of Heat and Mass Transfer* **131**(3) (2009), 033106 (9 pages), DOI: 10.1115/1.3056479.

[4] S. U. S. Choi, Z. G. Zhang, P. Keblinski and H. S. Nalwa, Nanofluids, *Encyclopedia of Nanoscience and Nanotechnology* **6** (2004), 757 – 737, American Scientific, Los Angeles, Calif., USA.

[5] S. K. Das, S. U. S. Choi and H. E. Patel, Heat transfer in nanofluids – A review, *Heat Transfer Engineering* **27**(10) (2006), 3 – 19, DOI: 10.1080/01457630600904593.

[6] E. O. Fatunmbi and S. O. Salawu, Analysis of hydromagnetic micropolar nanofluid flow past a nonlinear stretchable sheet and entropy generation with Navier slips, *International Journal of Modelling and Simulation* **42**(3) (2022), 359 – 369, DOI: 10.1080/02286203.2021.1905490.

[7] S. Hazarika and S. Ahmed, Material behaviour in micropolar fluid of Brownian motion over a stretchable disk with application of thermophoretic forces and diffusion-thermo, *Journal of Naval Architecture and Marine Engineering* **18**(1) (2021), 25 – 38, DOI: 10.3329/jname.v18i1.52518.

[8] S. P. Jeevandhar, V. Kedla, N. Gullapalli, S. K. Thavada, Free convective flow of water/ethylene glycol based micropolar nanofluid over a shrinking sheet, *Biointerface Research in Applied Chemistry* **11**(5) (2021), 12596 – 12605, DOI: 10.33263/BRIAC115.1259612605.

[9] M.-S. Liu, M. C.-C. Lin, I.-T. Huang and C.-C. Wang, Enhancement of thermal conductivity with carbon nanotube for nanofluids, *International Communications in Heat and Mass Transfer* **32**(9) (2005), 1202 – 1210, DOI: 10.1016/j.icheatmasstransfer.2005.05.005.

[10] P. Loganathan and N. G. Stepha, Chemical reaction effect on forced convective heat and mass transfer flow of micropolar fluid past a continuously moving porous plate in the presence of radiation, *International Journal of Heat and Technology* **30**(2) (2012), 107 – 144, DOI: 10.18280/ijht.300215.

[11] P. Loganathan and N. G. Stepha, Thermophoresis and mass transfer effects on flow of micropolar fluid past a continuously moving porous plate with variable viscosity and heat generation/absorption, *Asia-Pacific Journal of Chemical Engineering* **8** (2013), 870 – 879, DOI: 10.1002/apj.1732.

[12] F. Mabood, Md. Shamshuddin and S. R. Mishra, Characteristics of thermophoresis and Brownian motion on radiative reactive micropolar fluid flow towards continuously moving flat plate: HAM solution, *Mathematics and Computers in Simulation* **191** (2022), 187 – 202, DOI: 10.1016/j.matcom.2021.08.004.

[13] K. Rafique, H. Alotaibi, T. A. Nofal, M. I. Anwar, M. Misiran and I. Khan, Numerical solutions of micropolar nanofluid over an inclined surface using keller box analysis, *Journal of Mathematics* **2020** (2020), Article ID 6617652, 13 pages, DOI: 10.1155/2020/6617652.

[14] A. Rapits, Flow of a micropolar fluid past a continuously moving plate by the presence of radiation, *International Journal of Heat and Mass Transfer* **41**(18) (1998), 2865 – 2866, DOI: 10.1016/S0017-9310(98)00006-4.

[15] K. Singh, A. K. Pandey and M. Kumar, Numerical solution of micropolar fluid flow via stretchable surface with chemical reaction and melting heat transfer using Keller-Box method, *Propulsion and Power Research* **10**(2) (2021), 194 – 207, DOI: 10.1016/j.jppr.2020.11.006.

[16] V. M. Soundalgekar and H. S. Takhar, Flow of micropolar fluid past a continuously moving plate, *International Journal of Engineering Science* **21**(8) (1983), 961 – 965, DOI: 10.1016/0020-7225(83)90072-1.

[17] T. Tyler, O. Shenderova, G. Cunningham, J. Walsh, J. Drobnik and G. McGuire, Thermal transport properties of diamond-based nanofluids and nanocomposites, *Diamond and Related Materials* **15**(11-12) (2006), 2078 – 2081, DOI: 10.1016/j.diamond.2006.08.007.

[18] W. Yu, D. M. France, J. L. Routbort and S. U. S. Choi, Review and comparison of nanofluid thermal conductivity and heat transfer enhancements, *Heat Transfer Engineering* **29**(5) (2008), 432 – 460, DOI: 10.1080/01457630701850851.